

# Highly Confined Optical Modes in Nanoscale Metal-Dielectric Multilayers

Ivan Avrutsky<sup>1\*</sup>, Ildar Salakhutdinov<sup>1</sup>, Justin Elser<sup>2</sup>, Viktor Podolskiy<sup>2</sup>

<sup>1</sup>*Department of Electrical and Computer Engineering, Wayne State University, Detroit, Michigan 48202*

<sup>2</sup>*Department of Physics, Oregon State University, Corvallis, Oregon 97331*

We show that a stack of metal-dielectric nanolayers, in addition to the long- and short-range plasmons, guides also an entire family of modes strongly confined within the multilayer – the bulk plasmon modes. We propose the classification scheme that reflects specific properties of these modes. We report experimental verification of the bulk plasmon modes by measuring modal indices in a structure made of three pairs of silica(~29nm)/gold(~25nm) layers.

PACS numbers: 42.25.Bs, 42.82.Et, 73.20.Mf, 73.21.Ac

A thin dielectric layer surrounded by metallic claddings is known to support the gap plasmon – a guided mode with large modal index and deep sub-wavelength field confinement [1]. In this paper we show that a stack of metal-dielectric nanolayers guides an entire family of modes strongly confined within the multilayer – the bulk plasmon modes. The bulk modes have very short penetration depth into dielectric claddings. Their modal indices are typically large in absolute value and may be both positive and negative [2]. We propose a classification scheme that reflects specific properties of these modes. Finally, we report experimental verification of the bulk plasmon modes based on measuring modal indices in a structure made of three pairs of silica(~29nm)/gold(~25nm) layers.

The penetration depth  $L_{cl}$  of the guided mode field into a cladding is defined by vacuum wavelength  $\lambda$ , the modal index  $n^*$ , and the cladding permittivity  $\epsilon_{cl}$ :  $L_{cl} = \lambda / 2\pi \sqrt{n^{*2} - \epsilon_{cl}}$ .

In a structure with a given  $\epsilon_{cl}$ , the larger the modal index, the shorter the penetration depth is, which typically leads to stronger mode confinement. In all-dielectric waveguides, the modal index is always smaller than the core index, which makes such structures inappropriate for deep sub-wavelength light confinement. Practically, the most tightly confined mode would be supported by a silicon-on-insulator (SOI) waveguide with silicon core ( $n \approx 3.5$ ) and silica (or even vacuum) claddings [3].

Surface plasmon polaritons (SPP) [4] propagating along the interface between media with permittivities of different sign (metal and dielectric) are often considered as promising candidates for development of waveguides with strongly confined modes. The plasmon's modal index is determined by the permittivities of metal  $\epsilon_m$  and dielectric  $\epsilon_d$ :  $n_{SPP}^* = \sqrt{\epsilon_d \epsilon_m / (\epsilon_d + \epsilon_m)}$ . Typically, for most of practically important structures in the visible and near infrared spectral region, the permittivity of metal takes on large negative values  $|\epsilon_m| \gg \epsilon_d$ . This leads to sub-wavelength field penetration depth into metal, while the penetration into the dielectric can be as large as several wavelengths. Thus, for surface plasmons, the light intensity distribution across the interface is well beyond the nanoscale. A remarkable exception is the case of resonant surface plasmons [5] when dielectric permittivities of materials at different sides of the interface are exactly opposite one to another:  $\epsilon_m + \epsilon_d \rightarrow 0$  and thus  $n^* \rightarrow \infty$ . In homogeneous media, the field distribution of the resonant surface plasmon is expected to be confined

infinitely close to the interface. Actual scale of the field distribution is defined by the applicability of the concept of dielectric permittivity, that is, by the discrete atomic structure of materials. At optical frequencies, the resonant plasmons are possible if the dielectric has huge optical gain [6].

A metallic film of thickness  $t_m$  between dielectric claddings supports SPPs at each metal-dielectric interface. When the interfaces are brought sufficiently close to another, coupling between the individual plasmons leads to formation of symmetric and anti-symmetric film modes known as long- and short-range plasmons (LRP and SRP) [7, 8]. The coupling leads to splitting of the dispersion characteristics of the film modes. The modal index of the LRP is reduced compared to SPP approaching the index of the dielectric claddings:  $n_{LRP}^* \approx \sqrt{\epsilon_d + (\pi_m / \lambda)^2 ((\epsilon_d - \epsilon_m) \epsilon_d / \epsilon_m)^2}$ , and its field penetration depth into the claddings becomes larger accordingly. The modal index of the SRP is higher than that of the surface plasmons:  $n_{SRP}^* \approx \sqrt{\epsilon_d + (\lambda / \pi_m)^2 (\epsilon_d / \epsilon_m)^2}$ , yielding the confinement scale  $L_{SRP} = t_m + 2L_{cl} \approx t_m (1 + |\epsilon_m| / \epsilon_d)$ . Even though the metal film thickness can be within the nanoscale (10nm), the overall field distribution of both LRP and SRP is typically extended to quite a macroscopic scale. The modal indices of SRP and LRP in fused silica ( $\epsilon_d = 1.444^2 \approx 2.085$  [9]) / gold ( $\epsilon_m = -114.5 + 11.01i$ , [10]) system at  $\lambda = 1550\text{nm}$  as functions of metal thickness are shown in the first column of Fig. 1.

The splitting of modal index (and other dispersion characteristic) resulting from mode coupling is a universal property of optical waveguides, and it is an electromagnetic analog of energy level splitting in quantum mechanics. In fact, the modes in a multilayer composite can be related to the combination of surface modes at individual metal-dielectric interfaces, which are shifted and split due to the coupling. When two thin metallic films are brought close to each other, the LRPs and SRPs in these films start to interact with each other, leading to the splitting between their modal indices. Accordingly, the four modes of the double-film system will differ by their symmetry across metallic films and dielectric gap between the films. The mode with anti-symmetric magnetic field distribution across the dielectric gap experiences the cut-off when the gap thickness becomes of the order of  $\lambda / 2\sqrt{\epsilon_d}$ . This mode therefore does not exist in nanoscale structures. The mode with symmetric field distribution across the dielectric gap, the gap plasmon, survives, and its modal index increases as the gap becomes

thinner. For the case of a nanoscale dielectric gap of thickness  $t_d$  between infinitely thick metallic claddings, the modal index  $n_{GP}^*$  of gap plasmon

$$n_{GP}^* \approx \sqrt{\varepsilon_d + \frac{1}{2} \left( \frac{\lambda}{\pi d} \varepsilon_d \right)^2} + \sqrt{\left( \frac{\lambda}{\pi d} \varepsilon_d \right)^2 (\varepsilon_d - \varepsilon_m) + \frac{1}{4} \left( \frac{\lambda}{\pi d} \varepsilon_d \right)^4} \quad (1)$$

is inversely proportional to the gap size. Note that the modal index of the gap plasmon greatly exceeds that of the short-range plasmon, providing truly nanoscale mode confinement. Similar modes exist also in a gap between sharp metallic wedges [11]. Exact dispersion equations for modes in a gap between metallic claddings have been proposed in [12]. The modal indices of the coupled gap plasmons, SRP, and LRP in double-film structure are illustrated in Fig. 1.

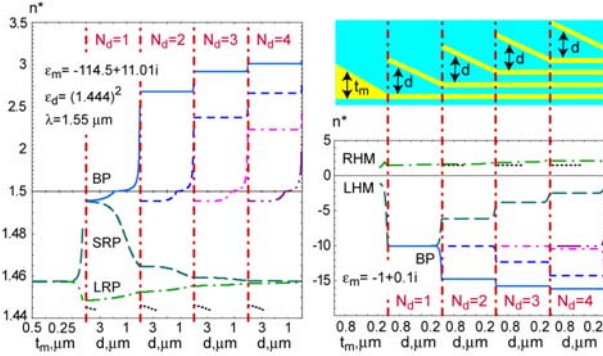


FIG. 1. Evolution of coupled SPP modal indices in the layered materials with dielectric claddings for  $|\varepsilon_m| > \varepsilon_d$  (left) and  $|\varepsilon_m| < \varepsilon_d$  (bottom right). System geometries are schematically shown in top-right inset, where blue and yellow regions represent dielectric and metal layers. Graphs at the left correspond to Au/SiO<sub>2</sub> composite considered in this work; graphs at the right represent its “negative index” counterpart with  $\varepsilon_m = -1 + 0.1i$  and  $\varepsilon_d = 1.444^2$ ;  $\lambda = 1550$  nm. First vertical portion of the figure illustrates the appearance of SRP/LRP doublet as a result of splitting between two SPPs (left) and as a result of mode/anti-mode formation (right). Other vertical portions illustrate the evolution of the modes in a layered structure when a metal layer is being gradually brought closer to the nanolayer stack.

As more layers are added to the structure, the collective interaction of SPPs leads to the mutual repulsion of modal indices. The modes originating from SPP combinations with asymmetric magnetic field distributions across the dielectric layers experience cut-off, while the gap plasmons survive, and contribute to the emergence of high-index supermodes, strongly confined to the bulk of the layered metamaterial. Since these bulk supermodes originate from repulsion of the gap plasmons, the total number of bulk modes is equal to the number of dielectric layers  $N_d$  in the multilayer. In addition, the entire multilayer may support surface modes at the interfaces with the dielectric claddings. Similar to SPP, these surface supermodes typically have poor confinement, and in case of symmetric claddings form LRP and SRP.

The surface modes behave fundamentally different when  $|\varepsilon_m| < \varepsilon_d$ . Although a single interface in this case does not support a SPP, a sufficiently thin film of negative-permittivity medium supports two modes with identical field

distribution ( $TM_0$ ) but different “handedness” – the relation between the directions of electric and magnetic fields and wavevector of the mode [2, 13] (Fig. 1, at the right). One of these modes is a direct “right-handed” analog of a long-range plasmon. The other one is its negative-index “left-handed” counterpart. While the analogy is not complete, negative index medium is often called optical anti-matter [14]. The  $TM_0$  mode doublet at close to the cut-off condition can therefore be considered as an example of formation of optical mode/anti-mode pair. Further analogy is seen in the formation of an *anti-symmetric* left-handed gap plasmon in a dielectric gap between metallic claddings when  $|\varepsilon_m| < \varepsilon_d$  [2, 15, 16]. Similar to the case of  $|\varepsilon_m| > \varepsilon_d$ , absolute value of the modal index for the left-handed waves increases as the metal interfaces get closer. Naturally, such an increase of the absolute value of the modal index is accompanied by stronger mode confinement.

The evolution of modal indices of guided right- and left-handed modes supported by thin multilayer films with dielectric claddings is illustrated in Fig. 1. Note that the repulsion of indices becomes significant when layers become sufficiently thin so that the gap plasmons in different dielectric layers substantially overlap with each other. Figs. 2 and 3 further summarize the modal indices of metal-dielectric composites with 25nm layers and dielectric claddings, realized in our experiment.

Optical losses of the bulk plasmon modes in multilayers are larger than losses of surface plasmons. Nevertheless, these modes are of significant interest to nanophotonics due to extremely strong field confinement. Besides light guiding by sub-wavelength structures, nanoscale multilayers with appropriately patterned films are promising candidates for development of metamaterials with negative refractive index [16-21], as well as for development of nano-sensors.

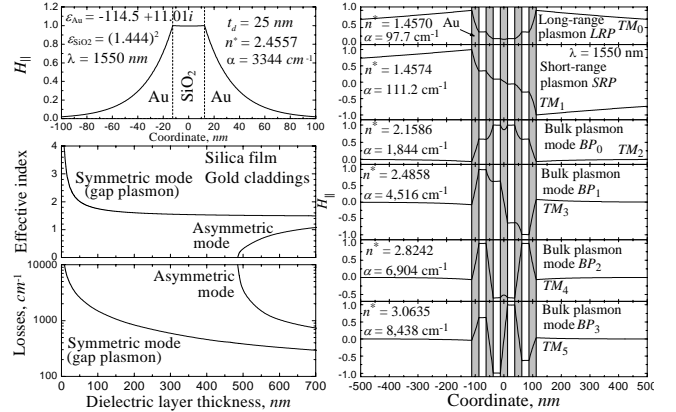


FIG. 2. Field profile (strength of magnetic field versus coordinate across the structure) for a gap plasmon and its effective index and losses as a function of the dielectric layer thickness (left). Profiles of modes supported by a nanoscale multilayer of 4 silica layers and 5 gold layers between silica claddings (right).

The traditional classification scheme for transverse electromagnetic modes in multilayers relies on the number of nodes in the field distributions. Accordingly, the SPP

supported by a single interface is a  $TM_0$  mode. The LRP and SRP supported by a thin metal film are labeled as  $TM_0$  and  $TM_1$  modes. The gap plasmon is a  $TM_0$  mode. Such a mode labeling scheme is perfect for the dielectric waveguides but causes some confusion when applied to nanoscale metal-dielectric structures. It is a bit inconvenient that the same label  $TM_0$  is designated to rather different electromagnetic excitations such as surface plasmons, long-range film plasmons, and the gap plasmons. Moreover, two modes of the left-handed metal strip are both  $TM_0$  waves. Further inconvenience is that essentially the same mode – the gap plasmon – is labeled  $TM_0$  in the structure with metallic claddings, and it becomes a  $TM_2$  mode in a structure with dielectric claddings, two thin metallic layers, and the guiding dielectric layer.

Once the highly confined volume modes and the film-plasmon-type modes have distinct properties, it is reasonable to label them differently. In particular, in a structure with large number of layers, the bulk mode with relatively smooth profile is reasonable to call the fundamental bulk plasmon mode  $BP_0$ . In the traditional numbering scheme this is a  $TM_2$  mode because it has two nodes close to the interfaces with the claddings. Accordingly, the bulk mode of order  $n$  ( $BP_n$ ) would be labeled as  $TM_{n+2}$  in the traditional classification. The labels such as  $LRP$  and  $SRP$  should be reserved for the modes with intensity maxima at multilayer-cladding interfaces which typically have large penetration depth into the dielectric claddings. When dielectric claddings have different permittivities, the labels  $LRP$  and  $SRP$  become rather senseless. Instead, conventional titles such as SPP bounded to particular interfaces will be more appropriate.

To illustrate the proposed classification scheme, Fig. 2 at the right shows the complete family of modes in a structure with  $N_d=4$  dielectric and  $N_m=5$  metallic layers (all the layers are 25 nm thick). The structure supports the long-range plasmon ( $LRP=TM_0$ ), the short-range plasmon ( $SRP=TM_1$ ), and four bulk plasmon modes ( $BP_0\dots BP_3=TM_2\dots TM_5$ ). Both LRP and SRP show large penetration into the claddings. In contrast, the bulk plasmon modes are confined within the multilayer with minor fraction of optical power propagating in the claddings. The fundamental bulk mode  $BP_0$  has relatively smooth field profile. For the highest order bulk mode, the field distribution reveals fast oscillations so that it has opposite signs in neighboring dielectric layers. Note that the modal indices of the bulk plasmon modes can be several times higher than the refractive index of the dielectric material in the multilayer. The origin of this surprising behavior is in the coupling-induced repulsion of the modal indices of individual gap plasmons discussed above.

The modal indices of guided modes in a multilayer with alternating 25nm thick layers of gold and silica are shown in Fig. 3. As predicted, the number of bulk modes is equal to the number of dielectric layers, and the maximal achievable modal index increases with the number of layers increasing. For any given number of layers, modes of higher order have larger losses and larger modal index. Assuming the number of layers is approaching infinity  $N\rightarrow\infty$ , we find the dispersion relation for the highest and the lowest order bulk plasmon mode ( $BP_N$  and  $BP_0$ ) by setting periodical boundary

conditions and requiring that the magnetic field strength has a node in the middle of every metal layer ( $BP_N$ ) or does not have such a node ( $BP_0$ ):

$$\tanh\left(\frac{\pi_m}{\lambda}\sqrt{n_{BP_N}^* - \varepsilon_m}\right)\tanh\left(\frac{\pi_d}{\lambda}\sqrt{n_{BP_N}^* - \varepsilon_d}\right) + \frac{\varepsilon_d}{\varepsilon_m}\sqrt{\frac{n_{BP_N}^* - \varepsilon_m}{n_{BP_N}^* - \varepsilon_d}} = 0 \quad (2)$$

$$\tanh\left(\frac{\pi_d}{\lambda}\sqrt{n_{BP_0}^* - \varepsilon_d}\right) / \tanh\left(\frac{\pi_m}{\lambda}\sqrt{n_{BP_0}^* - \varepsilon_m}\right) + \frac{\varepsilon_d}{\varepsilon_m}\sqrt{\frac{n_{BP_0}^* - \varepsilon_m}{n_{BP_0}^* - \varepsilon_d}} = 0$$

For nanoscale thicknesses of the layers, equation (2) yields following approximation for the modal indices

$$n_{BP_N}^* \approx \sqrt{\varepsilon_d - \frac{\lambda^2}{\pi^2 t_d t_m} \varepsilon_m} \quad n_{BP_0}^* \approx \sqrt{\varepsilon_d \varepsilon_m (t_d + t_m)}. \quad (3)$$

Note that the wavelength disappears from the expression for the modal index of the fundamental mode and the equation becomes equivalent to the predictions of the effective medium theory. The highest order mode, although it has strong wavelength dependence, has larger modal index than a single gap plasmon provided that  $t_{d,m} \ll \lambda/\pi\sqrt{|\varepsilon_m|}$ . A particular case of the fundamental mode, the one with the smallest losses, was studied back in 50's [22]. SPPs supported by a structure consisting of few metal and dielectric thin films have been studied earlier [23]. Non-local corrections to the averaged permittivity in metal-dielectric nano-composites are reported in our recent paper [24].

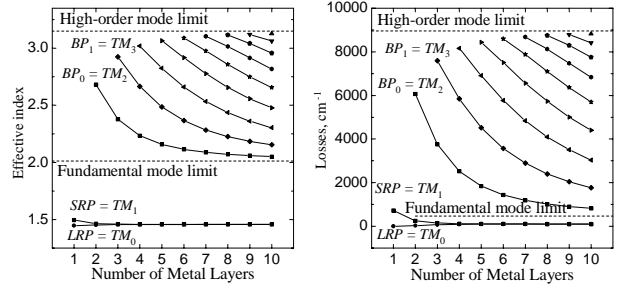


FIG. 3. Effective indices (left) and losses (right) for the modes in silica/gold multilayers. Dashed lines show the limits for the lowest order and highest order bulk modes in approximation of infinite number of layers (2).

For the gold-silica multilayers with  $t_d=t_m=25$ nm, numerical solution of (2) gives  $\text{Re}(n_{BP_N}^*) = 3.1488$  and  $\alpha = (4\pi/\lambda)\text{Im}(n_{BP_N}^*) = 8,959\text{cm}^{-1}$  – maximal possible values for the modal index and losses for the high-order bulk plasmon modes  $BP_n$ . Corresponding values for the fundamental bulk plasmon mode are  $\text{Re}(n_{BP_0}^*) = 2.0128$  and  $\alpha = (4\pi/\lambda)\text{Im}(n_{BP_0}^*) = 462.8\text{cm}^{-1}$ . These limits are shown in Fig. 3 by dashed lines stretched horizontally.

The variety of modes in a nanoscale metal-dielectric multilayer is relatively easy to predict and simulate numerically, but their experimental verification is challenging due to the deep sub-wavelength confinement and very high optical losses. In this paper we report, to the best of our knowledge, first experimental studies of guided modes in nanoscale metal-dielectric multilayers. To excite the high-

index modes, we used the evanescent light coupling scheme. High-index material such as silicon ( $n_{Si}=3.48$ ) was used to match the wavevector of light in free space to the wavevector of a guided mode. To access wider range of effective indices, semi-cylinder geometry instead of more traditional prism was used. Light from a fiber-coupled tunable (1490–1590nm) semiconductor laser (Photonics Inc.) was collimated using a 10× objective. The laser was tuned to the wavelength of 1550nm, which was verified by an optical spectrum analyzer (Hewlett-Packard HP70951B). The spectral width of the laser radiation was below the resolution of the spectrometer ( $<0.1\text{nm}$ ). The silicon semi-cylinder with a nanoscale metal-dielectric multilayer was mounted on a rotation stage so that the axis of the cylinder coincided with the axis of rotation. Angular reflection spectrum was measured, and datum were plotted as a function of the product  $n_{Si}\cdot\sin(\theta)$ , where  $\theta$  is the incident angle. In this scale, locations of the intensity minima directly indicate the modal indices of the guided modes excited through the evanescent light coupling.

The multilayer structure was designed to consist of three pairs of silica( $\sim 25\text{nm}$ )/gold( $\sim 25\text{nm}$ ). With two dielectric gaps between the three metal layers, the structure supports two bulk plasmon modes. The thickness of the layers was chosen to ensure that the effective indices of the bulk modes are in the comfortable for the measurement range ( $n^* < 3.0$ ). The experimental data are shown in Fig. 4 at the left. They indicate that the structure supports modes with effective indices 2.31 and 2.88 recognized as  $BP_0$  and  $BP_1$  modes. The overall structure was designed for measuring the modal indices of the bulk plasmon modes, while the surface plasmon mode at the interface with the substrate appears to be over-damped, and the surface plasmon at the interface with air has vanishing small evanescent coupling with the incident beam. By fitting the experimental data with numerically simulated angular reflection spectra, the best fit structure has been identified as Si-substrate/33nm-silica/24nm-gold/24nm-silica/26nm-gold/31nm-silica/24nm-gold

(in average, 29nm-silica/25nm-gold), which is reasonably close to the deposition target numbers. Fig. 4 also shows the modes' profiles in the experimental structure calculated using the best fit data for the thicknesses of the layers.

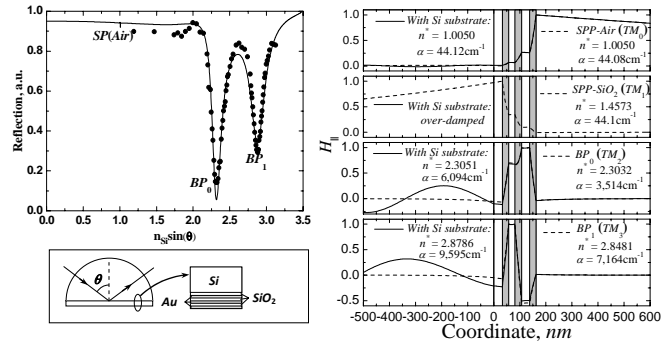


FIG. 4. Experimental reflection data for a silica/gold nanoscale multilayer (circles) and theoretical fit (solid line) indicating  $BP_0$  and  $BP_1$  modes (top left). The geometry of the experiment (bottom left). Simulated mode profiles in the experimental structure using the best fit thicknesses of the layers (right). Solid lines correspond to the structure with high-index silicon substrate. Dashed lines show mode profiles assuming the substrate is silica.

In conclusion, we analyzed  $TM$ -polarized modes supported by nanoscale metal-dielectric multilayers. We show that, in addition to the long-range and short-range plasmons supported by thin films, there are high-index guided modes strongly confined within the bulk of the multilayer. The dispersion relation is derived for the highest order and lowest order modes in approximation of infinite number of layers. New classification scheme is proposed for the modes supported in nanoscale metal-dielectric multilayers. High-index highly confined modes in a structure made of three pairs of gold( $\sim 25\text{nm}$ )/silica( $\sim 29\text{nm}$ ) layers are experimentally verified.

\* Corresponding author. E-mail avrutsky@eng.wayne.edu

<sup>1</sup> K. Tanaka, M. Tanaka, Appl. Phys. Lett. **82**, 1158-1160 (2003).

<sup>2</sup> A. Alu, N. Engheta, JOSA B, **23**, 571 (2006).

<sup>3</sup> Y. A. Vlasov, S. J. McNab, Optics Express **12**, 1622-1631 (2004).

<sup>4</sup> V. M. Agranovich, D. L. Mills, *Surface polaritons: electromagnetic waves at surfaces and interfaces* (Elsevier, New York, 1982).

<sup>5</sup> H. Raether, *Surface Plasmons on Smooth and Rough Surfaces and on Gratings* (Springer, Berlin, 1988).

<sup>6</sup> I. Avrutsky, Phys. Rev. B **70**, 155416 (2004).

<sup>7</sup> D. Sarid, Phys. Rev. Lett. **47**, 1927–1930 (1981).

<sup>8</sup> J.J. Burke, G.I. Stegeman, T. Tamir, Phys. Rev. B, **33**, 5186 (1986).

<sup>9</sup> E. D. Palik, *Handbook of Optical Constants of Solids* (Academic Press, New York, 1988).

<sup>10</sup> P. B. Johnson, R. W. Christy, Phys. Rev. B, **6**, 4370-4379 (1972).

<sup>11</sup> D.F.P. Pile, D.K. Gramotnev, M. Haraguchi, T. Okamoto, M. Fukui, J. Appl. Phys. **100**, 013101 (2006).

<sup>12</sup> T. Takano, J. Hamasaki, IEEE J. Quant. Elec. **QE-8**, 206-212 (1972).

<sup>13</sup> I. Shadrivov, A. Sukhorukov, Y. Kivshar, Phys. Rev. E **67**, 057602 (2003).

<sup>14</sup> J. B. Pendry, D. Smith, Physics Today **57**, 37 (2004).

<sup>15</sup> G. Shvets, Phys. Rev. B **67**, 035109 (2003).

<sup>16</sup> H. Shin, S. Fan, Phys. Rev. Lett. **96**, 073907 (2006).

<sup>17</sup> V. Podolskiy, E. Narimanov, Phys. Rev. B **71**, 201101 (R) (2005).

<sup>18</sup> J. B. Pendry, Phys. Rev. Lett. **85**, 3966 (2000).

<sup>19</sup> C. Luo, S. Johnson, J. Joannopoulos, J. Pendry, Phys. Rev. B **65**, 201104 (R) (2004).

<sup>20</sup> N. Fang, H. Lee, C. Sun, X. Zhang, Science **308**, 534-537 (2005).

<sup>21</sup> V. M. Shalaev, Nature Photonics **1**, 41-48 (2007).

<sup>22</sup> S. M. Rytov, Sov. Phys. JETP, **2**, 466–475 (1956).

<sup>23</sup> E. N. Economou, Phys. Rev. **182**, 539-554 (1969).

<sup>24</sup> J. Elser, V. A. Podolskiy, I. Salakhutdinov, I. Avrutsky, submitted to J. of Nanomaterials (2007).